Dynamics of Chain Aggregates of Carbon Nanoparticles in Isolation and in Polymer Films: Implications for Nanocomposite Materials

Rajdip Bandyopadhyaya,* Weizhi Rong, and Sheldon K. Friedlander

Department of Chemical Engineering, University of California at Los Angeles, Los Angeles, California 90095

Received March 26, 2004. Revised Manuscript Received June 1, 2004

Composite materials composed of polymers blended with reinforcing fillers play a major role in various technologies. An important example, commercial rubber, incorporates carbon black fillers, which significantly enhance mechanical properties such as Young's modulus and ultimate strength. The carbon black fillers consist of nanoparticle chain aggregates (NCAs). Because the mechanisms behind the filler effects are poorly understood, we have studied the dynamics of NCAs composed of carbon particles that we synthesize by laser ablation. In situ stretching of the NCA was carried out in the transmission electron microscope (TEM), first in the absence of a supporting polymer matrix and then embedded in a polymer film. The samples studied were first deposited across a micron-sized slit mounted on a commercial specimen holder in the TEM. For an isolated NCA, after initial reorientation and unfolding of the chain, a large strain led to its elongation, plastic deformation, and breakage, followed by fast recoil of the broken segments. On the other hand, a small strain could be partially recovered by subsequent contraction, displaying elastic behavior. Similar stretching and elastic behavior were observed for NCA embedded in polystyrene and neoprene films. Reorientation of chains within the film indicated load transfer to the former through the polymer matrix, which may contribute to the enhanced mechanical properties. The interactions within these nanocomposite films could be qualitatively arranged in the increasing order of polymer−polymer < particle−particle < polymer−particle. Finally, commercial carbon black fillers embedded in a poly(acrylic acid) polymer film also demonstrated stretching and reorientation similar to those of the NCA−polymer films. Our results therefore point to a possible mechanism of enhanced mechanical properties of carbon black nanocomposites: namely, separate contribution to the overall properties by the stretching and elastic properties of filler materials embedded in the polymer matrix.

Introduction

Composite materials containing nanoparticles as fillers form one class of nanocomposites.[1] Improved mechanical and electronic properties[2] of these materials form some of its advantages, which have resulted in their extensive study. The very high surface area of nanoparticles creates a large interfacial area between the fillers and the matrix in the composite. Properly controlled dispersion of particles in the matrix and particle−polymer interactions are crucial to the nanocomposite performance.[3,4] An important example is rubber reinforced by carbon black (CB) filler particles, which results in increased Young's modulus and tensile strength.[5] Although fillers constitute a significant amount (10−30% by weight) of the nanocomposite, the polymer−particle interaction and the mechanism of reinforcement are not well understood.[6]

Wang has reviewed the effect of polymer−particle and particle−particle interactions on mechanical properties of bulk rubber samples containing carbon or silica fillers.[7] To understand reinforcement, the variation in the *bound rubber* content (leading to one reinforcement mechanism) as a function of the specific surface area of the filler has been investigated.[8] The extent of amorphous domains on the CB surface also influences dynamic properties at low strain,[9] making this another significant filler parameter. However, most of these studies involve measurements on bulk specimens. Such bulk results provide answers to whether a material

* To whom correspondence should be addressed. Present address: Department of Chemical Engineering, Indian Institute of Technology Kanpur, Kanpur 208016, India. Tel.: 91-512-259 7697. Fax: 91-512-259 0104. E-mail: rajdip@iitk.ac.in, rajdip_ba@yahoo.com.

(1) Kornmann, X.; Lindberg, H.; Berglund, L. A. *Polymer* **2001**, *42*, 1303.
(2) Lonergan, M. C.; Severin, E. J.; Doleman, B. J.; Beaber, S. A.; Grubbs, R. H.; Lewis, N. S. *Chem. Mater.* **1996**, *8*, 2298.
(3) Wu, C. L.; Zhang, M. Q.; Rong, M. Z.; Friedrich, K. *Compos. Sci. Technol.* **2002**, *62*, 1327.
(4) Frogley, M. D.; Ravich, D.; Wagner, H. D. *Compos. Sci. Technol.* **2003**, *63*, 1647.
(5) Medalia A. I.; Kraus, G. Reinforcement of Elastomers by Particulate Fillers. In *Science and Technology of Rubber*; Mark, J. E., Erman, B., Eirich, F. R., Eds.; Academic: New York, 1994.
(6) Mark, J. E. *J. Phys. Chem. B* **2003**, *107*, 903.
(7) Wang, M. *Rubber Chem. Technol.* **1998**, *71*, 520.
(8) Wolff, S.; Wang, M.; Tan, E. *Rubber Chem. Technol.* **1993**, *66*, 163.
(9) Tricas, N.; Vidal-Escales, E.; Borros, S.; Gerspacher, M. *Compos. Sci. Technol.* **2003**, *63*, 1155.

10.1021/cm040049u CCC: $27.50
Published on Web 07/13/2004

performs well, but to explain reinforcement, one has to relate the properties to phenomena at much smaller length scales.

Also important are the surface structure and chemistry of individual CB nanoparticles, typically 5−30 nm in diameter. Studies at the primary particle level indicate that CB surfaces may be rough and even fractal[10] and the active surface sites may permit specific binding of polymers, hence leading to reinforcement.[11]

There are other hierarchical forms of the structure of CB fillers. These fillers are made by an aerosol synthesis route, whereby they form aggregate structures (typically 300 nm to 3 μm in dimension)[12] composed of individual (primary) nanoparticles, which are attached to their immediate neighbors through necklike regions formed by solid-state bonding. Furthermore, depending on the time−temperature history of the aerosol reactor, the aggregates can form loosely connected structures called agglomerates, which do not have a solid-state bond between them. The bonding between the particles in the neck region may be strong as a result of covalent forces but can decrease to weak van der Waals forces within the agglomerate.[13] In the manufacture of nanocomposite materials, *agglomerates* are broken down to smaller structures, typically to the size of aggregates, when the filler is blended mechanically with the rubber polymer.[14] Hence, the energy holding the particles and aggregates in the final product depends on both the formation and processing conditions. It is likely that a continuous spectrum of particle−particle bond energies ranging from van der Waals to covalent values determines the structure and mechanical properties of reinforcing fillers, and hence their effects on nanocomposites.

The filler structures described above are incorporated into a polymer matrix; aggregates are often comparable in size or larger than the polymer molecules, from which they differ fundamentally. It is not known whether standard theories of mechanical behavior can be extrapolated to length scales of nanocomposites.[4] One of the objectives of the present work is to experimentally investigate dynamic processes at the intermediate length scales of aggregates, which lie between bulk specimens and primary particles. The methods developed to study these phenomena may eventually make it possible to measure the distribution of bond energies that hold particles and aggregates together.

We have chosen a model system of nanoparticle chain aggregates (NCAs)[15] of carbon for our study. The NCAs are synthesized in our laboratory by laser ablation[16] and appear to be similar in structure to the CB fillers used in the manufacture of rubber tire tread.

NCAs are nearly linear structures with some side branches. In our first studies of their dynamic behavior,[15] they were shown to have an elastic like behavior under stretching. In studies by other investigators, poly(methyl methacrylate) polymer carrying silica particles (150 nm diameter) at 35−45 wt % were prepared.[17] Compared with randomly or regularly dispersed particles, *aggregated* silica produced a significant improvement of composite mechanical properties. It should be noted that the size of the primary particles used in these studies was much larger than those used as commercial fillers[5] or in studies conducted previously in our laboratory[18] and in the present work. In addition, the aggregates were produced by drying suspensions of silica nanoparticles, a process quite different from the aerosol synthesis used in industry. Our studies, in contrast, were made using NCA generated by laser ablation, an aerosol process.

Previous investigations have lacked direct microscopic observation of the evolution of the chain aggregates or the polymer under external loading. An objective of this study was to elucidate the mechanical behavior of carbon NCAs in isolation and embedded in polymer systems. To this end we have carried out transmission electron microscope (TEM) studies of the dynamics of these structures under tension.

Experimental Section

Carbon NCAs were produced by ablating a graphite target (spectroscopic grade, Ted Pella Inc.), using either an excimer laser[16] (Lambda Physik, model EMG101 MSC) with He as the carrier gas or a YAG laser (Hughes Aircraft Co., MDIVAD Laser Rangefinder) with Ar as the carrier gas. The average laser power was 100 mJ/pulse, with a pulse frequency of 10 Hz. A few NCAs in the gas exiting the laser ablation chamber were deposited either on a Formvar-coated TEM grid made of Cu or on a nanostructure manipulation device (NSMD)[19] designed and built in our laboratory. The device contains a 2−4 μm wide horizontal slit on a 3 mm diameter deformable alloy (38.1 wt % Pb−Sn) disk. The NCAs deposited across this slit thereby formed a bridge.

By insertion of this NSMD (carrying several NCA bridges) into the commercial elongation specimen holder of a TEM, it was possible to widen or narrow the slit width. Each end of the NCA remained adhered firmly to the respective edges of the slit during this manipulation. These maneuvers resulted in either an increasing or a decreasing tension on the NCA, and the dynamics was followed in situ with the TEM. The TEM (JEOL, model JEM-100 CX) was operated at an accelerating voltage of 100 keV with magnifications ranging from 6300 to 130 000.

Figure 1a summarizes three methods used for making polymer−NCA films, depending on the polymer used and whether a TEM grid or a NSMD was used for making a film sample. We have used polymers with different characteristics, namely, polystyrene (PS, which has a high elastic modulus and low breakage strain) and neoprene (which has a low elastic modulus and high breakage strain and behaves as a rubber).

In the first method, a TEM grid containing predeposited NCA was placed on an absorbing paper. A drop of a PS solution (M_w= 18 700, Sigma-Aldrich) in toluene (Fisher Scientific; PS concentration = 5.4 wt %) was put on the grid with a syringe. The drop was very quickly absorbed because it was in contact with the absorbing paper underneath. With simultaneous evaporation of the remaining toluene, a PS film containing embedded NCA formed on the grid.

(10) Heinrich, G.; Kluppel, M.; Vilgis, T. A. *Curr. Opin. Solid State Mater. Sci.* **2002**, *6*, 195.
(11) Donnet, J. B. *Compos. Sci. Technol.* **2003**, *63*, 1085.
(12) Hess, W. M.; Herd, C. R.; Sebok, E. B.; Swartz, L. A. *Kaut. Gummi Kunstst.* **1994**, *47*, 328.
(13) Friedlander, S. K. *Smoke, Dust, and Haze*; Oxford University Press: New York, 2000.
(14) Gerspacher, M.; O'Farrell, C. P.; Yang, H. H. *Kautsch. Gummi Kunstst.* **1994**, *47*, 349.
(15) Friedlander, S. K.; Jang, H. D.; Ryu, K. H. *Appl. Phys. Lett.* **1998**, *72*, 173.
(16) Ogawa, K.; Vogt, T.; Ullmann, M.; Johnson, S.; Friedlander, S. K. *J. Appl. Phys.* **2000**, *87*, 63.
(17) Pu, Z.; Mark, J. E.; Jethmalani, J. M.; Ford, W. T. *Chem. Mater.* **1997**, *9*, 2442.
(18) Suh, Y. J.; Friedlander, S. K. *J. Appl. Phys.* **2003**, *93*, 3515.
(19) Suh, Y. J.; Prikhodko, S. V.; Friedlander, S. K. *Microsc. Microanal.* **2002**, *8*, 497.

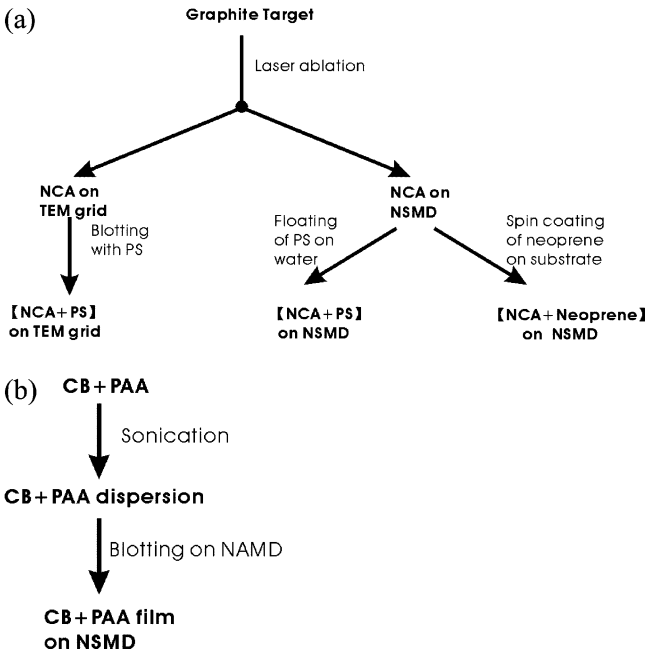

Figure 1. Scheme showing the synthesis of nanocomposite films: (a) NCA−polymer; (b) CB−polymer.

In the second method, a solution of PS in toluene (PS concentration = 5.4 wt %) was sprayed from a micropipet onto the surface of water taken in a beaker. A polymer film formed as a result of evaporation of toluene and remained floating at the air−water interface. With the help of a tweezer, the NSMD (containing predeposited NCA) was then immersed in water and placed under the floating film. Subsequently, the film was gently lifted onto the slit. Thus, we obtain a NCA-embedded PS film across the slit of the NSMD.

To make NCA-embedded neoprene films, a third method was employed. To this end, an aqueous dispersion of neoprene (Neoprene 750, Dupont) was spin coated on a glass substrate at 8000 rpm for 30 s. The neoprene film was dried overnight and then cut with a stainless steel blade. The cut portion of the film was easily detached from the glass substrate and then placed across the slit of the NSMD, containing predeposited NCA.

Figure 1b shows the method used for making CB−polymer films. First a dispersion was made by 10−15 min of sonication of commercial-grade CB (80 m^2/g specific surface area and 42 nm average particle size; Alfa-Aeser) in a solution of poly(acrylic acid) (PAA; 35 wt % aqueous solution of sodium salt of PAA, M_w=35 000, Sigma-Aldrich) to obtain a 0.4 wt % CB dispersion. A drop of the dispersion was then placed on the slit of a NSMD, and the excess liquid was removed by an absorbing paper to obtain a CB−PAA film covering the slit.

Results and Discussion

First, we discuss the dynamics of an individual carbon NCA for different extents of strain. Next, we examine the behavior of these NCAs in composite films of either PS or neoprene. Finally, we describe observations on CB−polymer films, as a way to relate the features of NCA to the actual commercial fillers in use.

Dynamics of an Individual NCA: Stretching under Large Strain. Figure 2 shows a typical carbon NCA, which is attached to two edges of the slit on the NSMD. The points S_1 and S_2 serve to identify the locus of the slit as it is stretched. The resultant increase in tension in the NCA causes it to gradually stretch from the straight, taut configuration in Figure 2a to a maximum stretched state in Figure 2d. The increase in the chain length can be followed through the evolving location of the points P and Q on the chain. Measurement of the distance PQ along the NCA gives a maximum strain of 37.4% from Figure 2a−d, before further stretching resulted in breakage of the NCA (Figure 2e). This therefore is the breaking strain in this case, which shows that NCAs can sustain a large strain. At this point the broken segments recoiled toward the attached ends. One part, in fact, collapsed and rearranged near the end marked S_1 in Figure 2e. These observations agree with those of our previous work.[16]

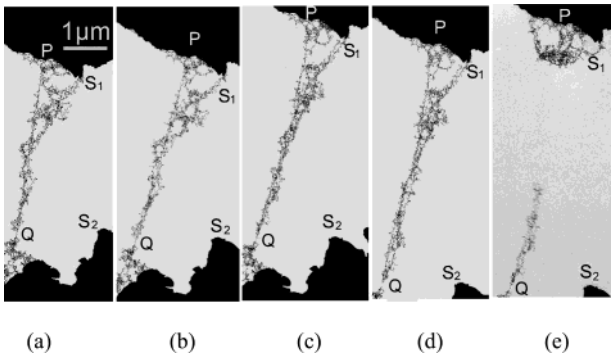

Figure 2. Stretching and recoiling of carbon NCA under large strain. The average strain rate was 5.4×10^{-3} s^{-1}. S_1 and S_2 are points on the edges of the slit on NSMD, which appear as dark areas in the images. PQ denotes a segment of the NCA. The scale bar applies to all images.

Stretching and Contraction under Large Strain. Figure 3 shows a sequence of steps in which the NCA is first stretched from Figure 3a−c. The configuration of the as-deposited chain in Figure 3a is quite folded. Stretching causes reorganization of the NCA by movement of the individual particles, resulting in a more straight and taut chain in Figure 3c. Stretching was stopped before reaching the breaking point, unlike that in Figure 2. Subsequently, the taut chain is allowed to contract as seen in Figure 3d,e, by bringing the two edges of the slit closer. The aim was to see whether the length of the chain decreases without any loss of the straight, taut configuration. Figure 3d, however, shows that the chain started to develop kinks over small length scales and partially lost its taut configuration. Further reduction in the distance of the slit edges in Figure 3e caused the chain to bend and form a loop with a large curvature, without much decrease in the contour length. The NCA had been stretched by almost 20% in length (along the segment PQ) to reach the state in Figure 3c. This, therefore, is too large a strain to observe reversibility; that is, the high strain initiates permanent deformation.

Stretching and Contraction under Small Strain. Application of the NCA in tires, however, utilizes rubber at much smaller deformations in comparison to breaking strains.[20] A strain of 0.1−10% can be considered a low strain.[9] Experiments under small strains are shown in Figure 4. It shows three images of the same segment of a chain whose length in the original, stretched, and contracted states are shown in Figure 4a−c. The lengths of the segment PQ in the three images are 524, 536,

(20) Payne, A. R. Dynamic Properties of Filler-loaded Rubbers. In *Reinforcement of Elastomers*; Krauss, G., Ed.; Interscience Publishers: New York, 1965.

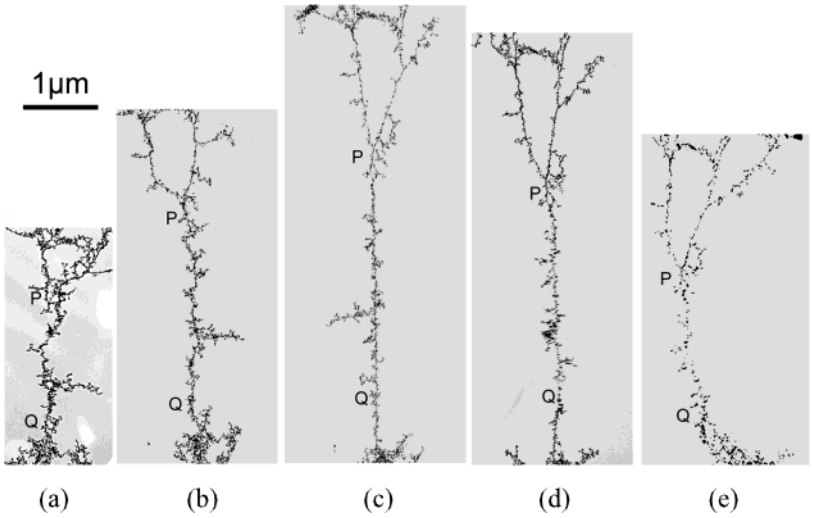

Figure 3. Stretching and contraction of carbon NCA under large strain. The average strain rate was 4.5×10^{-3} s^{-1} during stretching and 2×10^{-3} s^{-1} during contraction. The NSMD is not shown. PQ denotes a segment of the NCA. The scale bar applies to all images.

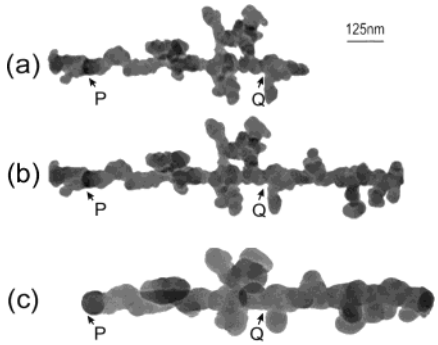

Figure 4. Stretching and contraction of carbon NCA under small strain. The NSMD is not shown. PQ denotes a segment of the NCA. The scale bar applies to all images.

and 529 nm, respectively. With a tensile strain of only 2.3% from Figure 4a,b (for the segment PQ), we find that locally about 60% of this tensile strain is recovered on contracting from part b to part c of Figure 4. This indicates a partial reversibility and is an indication of the elastic nature of these chains. On comparison of parts b and c of Figure 4, it is clear that the side branches have come closer to the main chain and the particles appear enlarged. This was also seen in other segments of the chain that do not appear in this figure. A probable reason for the enlargement is the exposure of the chain under the electron beam for almost 2 h, during the sequence of stretching and contraction. This is much longer than the time taken for conducting experiments at large strain, which were on the order of tens of minutes only. There have been similar reports of large swelling and shape changes in graphite (our NCA is also made from a graphite target) under electron beam irradiation in the TEM.[21]

Summary of Individual NCA Dynamics. The above observations are summarized in Figure 5a. When tension is applied to an isolated NCA, the behavior can be divided into a few steps. First, chain kinks on the scale of a few particle diameters are straightened by rotation and/or sliding at particle−particle interfaces. This has been observed in Figure 3a−c. We refer to this step in Figure 5a as reorganization of the folded chain into a straight, taut configuration. This includes overcoming the van der Waals force of attraction between nonneighboring particles on a folded chain.

Next, two possibilities are shown in Figure 5a. Application of a small tensile strain to the taut chain and subsequent reduction in tension cause the chain to contract (almost to the original length) without losing its straight configuration. This possibility has been illustrated in the images of Figure 4. It implies a partial reversibility of the strain under stretching and contraction and may explain the elastic nature of the NCA, under certain conditions. The second possibility in Figure 5a shows the effect of a very large strain applied by continuous stretching of the chain. Subsequently, this can lead either to breakage and recoil of the chain due to further stretching or to a permanent deformation on contraction. These two cases have been illustrated in Figures 2 and 3, respectively.

The above observations have been put together to construct a qualitative stress−strain curve shown in Figure 5b. This is in line with our previous observation[18] and extends it further to include some other features observed in the present experiments. Some components of this stress−strain diagram are similar to bulk samples of ductile materials.[22] Stage I (from A to B) corresponds to the reorganization step, where a small stress can cause the aggregate to unfold and result in a large change in its linear dimension. Next, stage II (section BC) shows the elastic region of the aggregate, where a comparatively larger stress is required to strain the NCA by a small amount, but the strain may be completely recovered; this region is reversible. Stress−strain curves similar to those of stages I and II have been measured for naturally occurring polymer fibers,[23] which consist of folded subunits in a long polymer molecule, akin to our NCA.

(21) Koike, J.; Pedreza, D. F. *J. Mater. Res.* **1994**, *9*, 1899.

(22) Hibbeler, R. C. *Mechanics of Materials*; Prentice Hall: Englewood Cliffs, NJ, 1997.

(23) Smith, B. L.; Schaffer, T. E.; Viani, M.; Thompson, J. B.; Frederick, N. A.; Kindt, J.; Belcher, A.; Stucky, G. D.; Morse, D. E.; Hansma, P. K. *Nature* **1999**, *399*, 761.

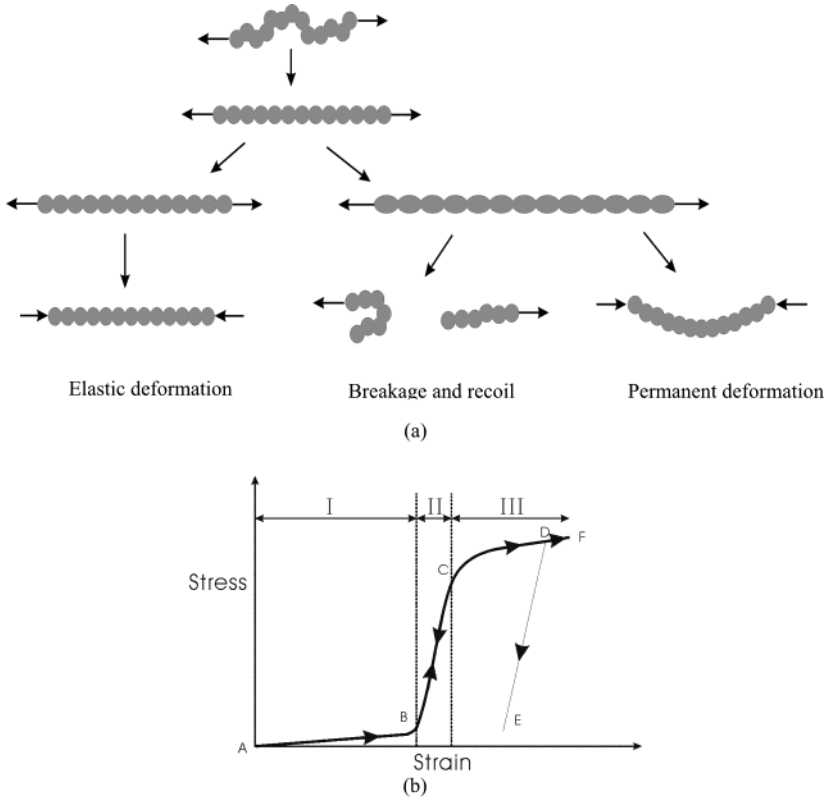

Figure 5. (a) Summary of different possible behaviors of an individual NCA based on experiments on dynamics of isolated NCA. (b) A qualitative stress−strain diagram for the NCA.

Finally, further strain leads to stage III (section CF), which is the region of permanent deformation. F is the point of breakage of the NCA. If, however, a contraction is initiated beforehand at point D, the behavior follows the segment from D to E. A part of the permanent deformation can be recovered, as seen between reduced strain values from Figure 3c,d.

Dynamics of a Polymer−NCA Film: Stretching of a PS−NCA Film. In this and the following sections, we discuss the dynamics of NCA embedded in PS and neoprene films. Our aim is to assess the role of NCA in these composites. First we take up the behavior of PS−NCA films. Figure 6 shows the effect of stretching of such a composite film in the NSMD. S_1 and S_2 are the two edges of the slit. The film appears as a long and narrow piece enclosing the NCA. Upon stretching, some branches of the NCA broke off successively in the region marked A, and finally the whole aggregate broke up in Figure 6c. Parts b and c of Figure 6 show only the region corresponding to that marked A in Figure 6a. The breakup of the NCA near its center in Figure 6b, instead of tearing loose from the polymer film, implies that the polymer−particle interaction is stronger than the particle−particle interaction.

Next we study the structure and also the dynamics of NCA embedded in a PS film under irradiation of the electron beam in a TEM. To this end, we first observe an as-deposited NCA on the TEM grid in Figure 7a. It shows the individual primary particles in the NCA and the overall structure of the chain. Subsequently, the PS film was deposited on the grid, in a manner discussed previously in the Experimental Section. Parts b−d of Figure 7 form a sequence of images from the same region of such a composite film on the grid, while it is

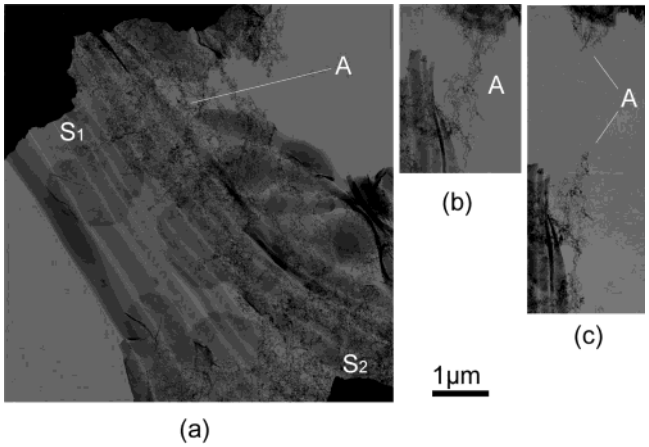

Figure 6. Stretching of a nanocomposite film of carbon NCA with PS. (a) Overall configuration of the film incorporating the NCA. The region marked A is shown in parts b and c, where the NCA stretches and then breaks. S_1 and S_2 denote two edges of the NSMD. The scale bar applies to all images.

exposed to a focused electron beam in the TEM, at a current density of 5×10^4 A m^{-2}. As a result of this irradiation, both the PS film and the NCA were exposed to the same conditions. The contrast in the images of Figure 7b−d was not very good because of the presence of this additional PS film. On continued irradiation, we find in Figure 7c that a hole developed in the PS film. The NCA, however, remained intact and did not break. This indicates that the polymer−polymer interaction strength is weaker than that of the particle−particle interaction. Finally, when the NCA also broke in Figure 7d, it remained attached to the polymer film and contracted in length. Thus, the contraction of the NCA

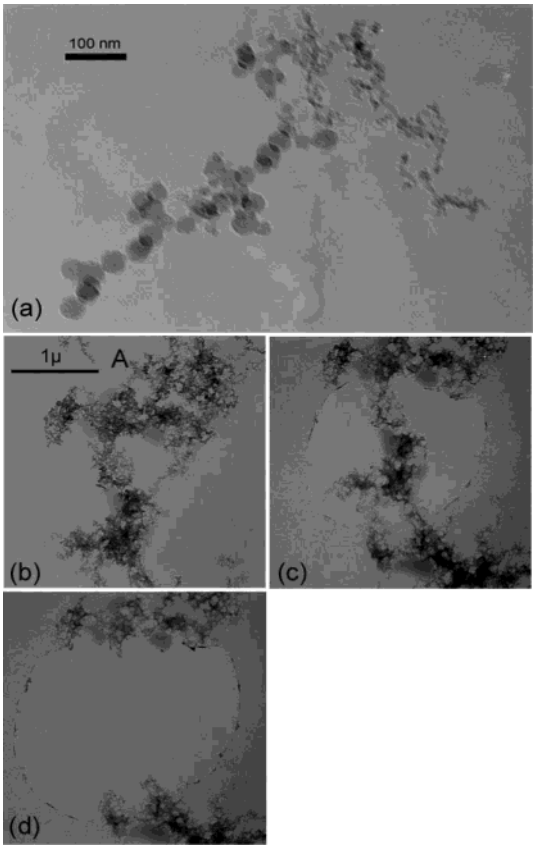

Figure 7. (a) Carbon NCA deposited on a Formvar-coated Cu−TEM grid showing primary particles and the overall chain structure. (b−d) Stretching of a nanocomposite film of carbon NCA with PS at a different location on the same grid as that in part a. A hole is formed in the PS matrix by electron irradiation from part b to part d, finally resulting in fracture and contraction of the NCA in part d. The scale bar in part b applies to images from parts b−d.

after breakage, observed earlier for isolated aggregates, occurs when it is embedded in the polymer film too. This means that the inherent elastic behavior of the NCA may contribute to reinforcement when present in the composite. Figure 7d also shows that the NCA did not pull out of the film after breakage. This once again proves that the polymer−particle interaction is stronger than the particle−particle interaction. Apparently, similar studies on the effect of electron beam irradiation and thermal treatment have been conducted on the structural evolution of metal nanoparticle embedded polymer films.[24] The author's aim in this, however, was to understand the different mechanisms leading to changes in the size and shape of the nanoparticles due to irradiation, namely, Ostwald ripening, particle restructuring, coalescence, and particle migration in the polymer matrix. On the other hand, our objective here was to observe the relative response of the polymer and the NCA under stress to assess their interaction strengths.

Stretching of a Neoprene−NCA Film. We now come to the observations on the structure and dynamics of NCA embedded in neoprene films. This is illustrated in Figures 8−10. Figure 8 shows a high-magnification image of the NCA−neoprene film in which the primary particles of the NCA can be seen. Although some

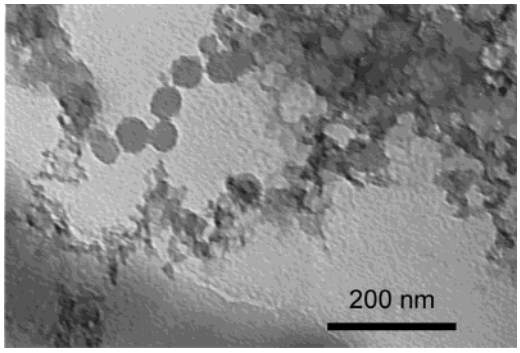

Figure 8. Nanocomposite film of carbon NCA with spin-coated neoprene, showing individual particles of NCA and bound rubber on the top right corner.

segment of the NCA is clearly visible, most of it is instead surrounded by neoprene, akin to a *bound rubber* phase. In the literature, the bound rubber phase has been hypothesized to be one reason for reinforcement because these rubber molecules are less mobile than free rubber and thereby increase the effective filler fraction.[25] Here the authors proposed different forms of bound rubber, namely, a rubber *shell* around individual filler particle and aggregates or rubber *occluded* and *trapped* by one or more aggregates. In experiments with a system of elastomeric blends, it has been indirectly inferred from neutron reflectivity and lateral force microscopy measurements that the elastomer chains adsorb on CB filler.[26] In another study, polyisoprene (chemically very similar to chloroprene, the main constituent of neoprene used by us) was found to form only a shell of rubber layer around fumed silica aggregates.[27] In contrast to these reports, from the micrograph in Figure 8, we directly observe a trapped and occluded phase of rubber, surrounding the NCA, as proposed elsewhere.[25]

Next, Figure 9 shows stretching of such a film containing NCA embedded in neoprene. Comparison of parts a and b of Figure 9 shows that the NCA reoriented during stretching, so that the side chain marked A and the adjoining segment contracted laterally. Simultaneously, the NCA also rotated by a small amount, so that a new side branch (marked C) appeared in Figure 9b. This implies that the externally applied tensile load was transmitted through the neoprene film to the NCA. Further stretching caused a big crack to form laterally across the sample (in a direction roughly perpendicular to the externally applied tensile force), which broke apart the film. Simultaneously, the NCA also fractured. Only a small portion of the NCA protruded out into the crack, but it did not pull apart from the neoprene film.

Finally, Figure 10 shows another NCA from a different region of the same sample as above. Although the NCA shows a thin section composed of very small primary particles, it did not break at that point during stretching. Instead, the NCA broke where the crack in the film (the same as in Figure 9) propagated rapidly.

(24) Heilmann, A. *Polymer Films with Embedded Metal Nanoparticles*; Springer: London, 2002.

(25) Kohls, D. J.; Beaucage, G. *Curr. Opin. Solid State Mater. Sci.* **2002**, *6*, 183.

(26) Zhang, Y.; Ge, S.; Tang, B.; Koga, T.; Rafailovich, M. H.; Sokolov, J. C.; Peiffer, D. G.; Li, Z.; Dias, A. J.; McElrath, K. O.; Lin, M. Y.; Satija, S. K.; Urquhart, S. G.; Ade, H.; Nguyen, D. *Macromolecules* **2001**, *34*, 7056.

(27) Ono, S.; Kiuchi, Y.; Sawanobori, J.; Ito, M. *Polym. Int.* **1999**, *48*, 1035.

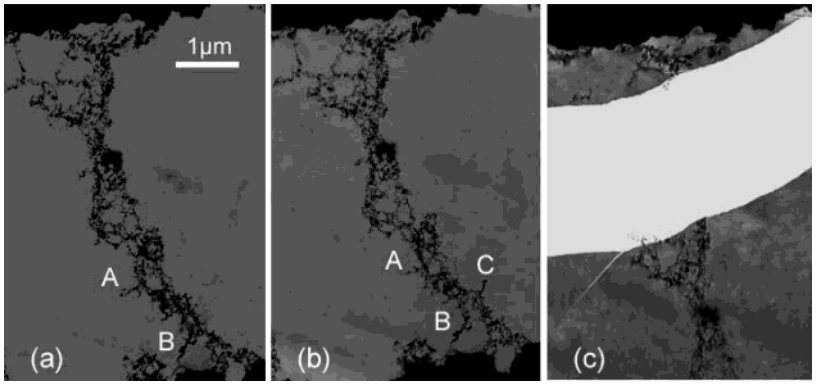

Figure 9. Stretching of a nanocomposite film of carbon NCA with neoprene showing reorientation of NCA from part a to part b with the appearance of side branch C and (c) formation of a crack on further stretching. Black areas denote two edges of the slit of the NSMD. The scale bar applies to all images.

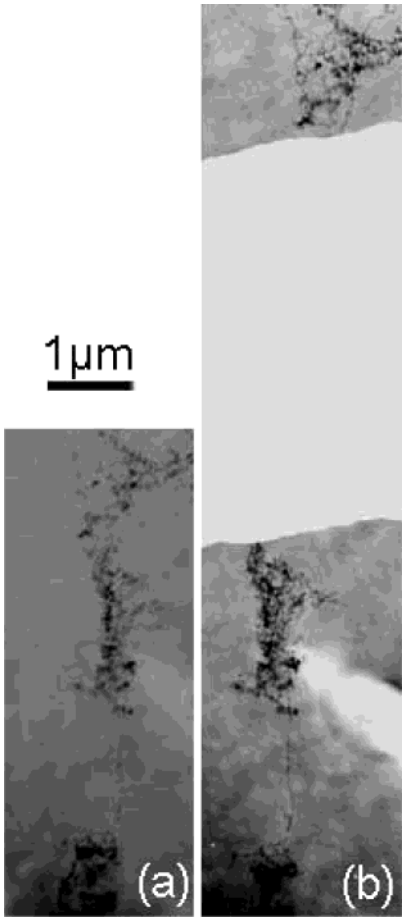

Figure 10. Stretching of a nanocomposite film of carbon NCA with neoprene, showing (a) a thin segment of the NCA and (b) formation of a crack in the film, not fracturing the thin segment. The scale bar applies to both images.

This suggests that the NCA seen here probably broke in a region where large shear stress was generated by the crack in the film (which propagated very fast laterally across the whole film on the NSMD slit); otherwise, it would have broken at the thin section. So, this means that the particle−particle interaction strength is larger than that of the polymer−polymer interaction for this polymer too.

Summary of Polymer−NCA Dynamics. From the above observations, we draw an overall picture of the nature of interactions between the polymer and NCA. This is summarized in Figure 11, which shows two

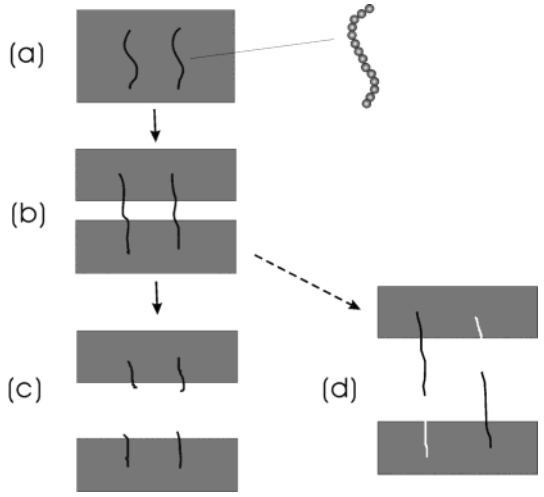

Figure 11. Schematic of the overall process of a polymer−NCA film under stretching.

NCAs in a polymer film, with the latter being shown by a shaded region. The particulate structure of the NCA is highlighted in a magnified view in Figure 11a. We make the following observations: (1) The polymer−polymer interaction is weak compared to the particle−particle interaction. As a result, upon stretching, the particle chain remains intact, whereas the polymer film fractures, as shown in Figure 11b. (2) The particle−particle interaction is weaker than the polymer−particle interaction, leading to breakage of particle chains (in Figure 11c) rather than their separation from the polymer matrix. The latter is shown as an alternative possibility in Figure 11d, which is not seen presently. This is desirable as far as the role of NCAs as reinforcement filler is concerned. They, therefore, form a strong bond with the polymer matrix. In fact, the carbon particles are hydrophobic and hence nonpolar, leading to a favorable interaction with both neoprene and PS, which too are only very weakly polar. In explaining reinforcement of rubber by fillers, previous workers have hypothesized that rubber−rubber interactions are not as significant compared to filler−filler and rubber−filler interactions, except when blends of two rubbers are used.[25] Our results are consistent with this observation.

Stretching of a CB−Polymer Film. Figure 12 shows the stretching of a nanocomposite film of CB in PAA on the NSMD. We see that the CB particles exist

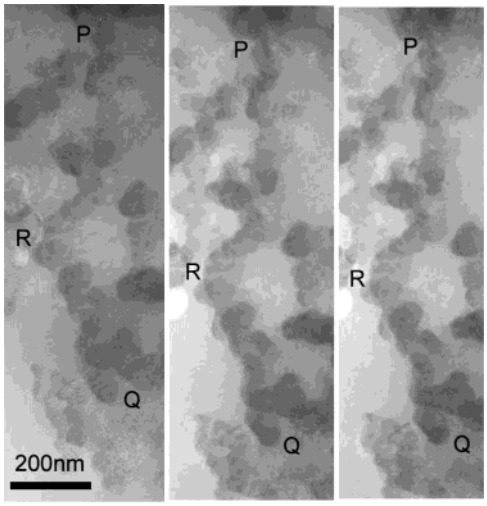

Figure 12. Stretching of a CB-embedded PAA nanocomposite film. The NSMD is not shown. PQ denotes a segment of the CB chain, while R is a point in the midsection of the chain. The scale bar applies to all images.

as a folded chain in the polymer matrix (Figure 12a). We found from TEM images (not shown) that the as-received CB is in the form of chainlike aggregates, which is the typical state of aggregation of carbon fillers used in practical applications.[5] These are structurally similar to our laser-generated carbon NCAs. On the basis of the initial configuration of the chain in Figure 12a, the tensile strain of the segment PQ is 3.7% in Figure 5c. We also find that the chain is unfolded, for example, at point R, where the angle subtended increases from 89° to 112°. This clearly shows for the first time to our knowledge the unfolding and stretching of CB chains in a polymer matrix.

Summary and Conclusions

NCAs of carbon were made by laser ablation of graphite. The dynamics of these chains was studied by in situ stretching and contraction in a TEM. Isolated NCAs behaved differently at large and small strains. After initial chain reorganization, large strains led to plastic deformation and breakage of the chain, with fast recoiling of the broken segments. On the other hand, for a small strain, successive stretching and contraction led to partial recovery of the tensile strain. This indicates the elastic nature of the NCA.

In the next step, the NCAs were incorporated in a PS or neoprene film and the motion of the aggregates was observed either by stretching of the film mechanically in the NSMD or by electron irradiation of a TEM grid. The tensile stress led to first the failure of the polymer film and then stretching and breakage of the NCA. In no instance did the NCA pull apart from the polymer matrix; instead, it broke apart, much like an isolated NCA. On the basis of these observations, we therefore rank the strength of the interactions in the following increasing order: polymer−polymer < particle−particle < polymer−particle. The NCA reoriented under strain, indicating a good load transfer through the polymer matrix. By and large, the elastic behavior of the NCA in the polymer matrix was similar to that of the isolated NCA.

CB fillers used for reinforcement of rubber also possess a chainlike structure made of individual particles. Although a detailed structure of the fillers depends on the original aerosol formation process, they are quite similar to the NCA made by us. Further experiments showed that commercial CB fillers embedded in a polymer film also undergo reorientation and stretching like the NCA. In general, properties of the nanocomposite depend on the interactions between the polymer and aggregates, which can be modified during blending of the two. However, our findings on the dynamics and elastic nature of the NCA, both in isolation and in the polymer matrix may still apply to carbon fillers too. This can point toward a possible mechanism of enhancement of elastic properties of rubber by these fillers. Previous studies of the viscoelasticity of reinforced rubber based on macroscopic measurements have shown different trends at small (less than 5−7%) and large strains.[14] Our present experiments on isolated NCA at different strains for the first time show this at microscopic length scales.

Acknowledgment. This research was sponsored in part by NSF Grants CTS 9911133 and CTS 9527999.

CM040049U